X-713-68-134

PREPRINT

NASA TM X-63279

CONTAMINATION MONITOR

JANUARY 1968

GSFC

GODDARD SPACE FLIGHT CENTER

GREENBELT, MARYLAND

X-713-68-134

CONTAMINATION MONITOR

Robert N. Sheehy
Spacecraft Technology Division

January 1968

GODDARD SPACE FLIGHT CENTER
Greenbelt, Maryland

CONTAMINATION MONITOR

Robert N. Sheehy
Spacecraft Technology Division

ABSTRACT

A self-contained optical-electronic instrument was flown on the AIMP-E satellite to detect contamination deposits on the instrument's sensor surface during launch, transfer trajectory, and insertion into a lunar orbit.

CONTENTS

ILLUSTRATIONS

CONTAMINATION MONITOR

INTRODUCTION

The contamination monitor flown on the AIMP-E satellite used established optical principles to determine the change in known reflective characteristics of the sampled surface.

The instrument consists of a reliable collimated light source projected through an illuminating lens onto the surface to be sampled. The reflected image is transmitted through a collimating lens which focuses on and illuminates the instrument's sensor-cell surface.

BACKGROUND

In April 1966, a contamination monitor was proposed to detect possible contamination deposits on the spacecraft surfaces during launch and continuing until last-stage separation.

The need for this instrument was established by flight results obtained from the AIMP-D spacecraft. The spacecraft performed well within predicted temperature ranges until the aspect angle of the sun was 30 degrees with respect to the spin axis. The spacecraft temperatures started to rise and continued to do so until the sun was perpendicular to the top cover. This condition occurred approximately 60 days after the spacecraft was in orbit. At that time the spacecraft exceeded its upper temperature limitations and went to a +60° C which contributed to the loss of the spacecraft battery. The thermal design engineer of the AIMP-D satellite performed an analysis and concluded that in order for the spacecraft to fly at this elevated temperature it would be necessary to double the effective solar absorptance and thermal emittance of the thermal control surfaces. To achieve this result the optical characteristics of the original coatings would have to be drastically altered or a contaminating film deposited on the surface. The possibility of contamination existed because the fourth stage rocket which was used to place the spacecraft in orbit was directly mounted to it. For the original mission, the solar aspect would have been restricted to small angles about the normal to the spin axis. Under these conditions if the top surface had been contaminated, the effect on spacecraft temperature would have been much less noticeable. For the actual mission, however, the sun's angle varied so that the effect of contamination would be significant as mentioned.

The design of AIMP-E, successor to AIMP-D, was modified so as to reduce the effect of possible changes in the thermal control properties of the top surface. However, it was of interest to the AIMP-E project manager to determine whether significant contamination does occur when the fourth stage rocket is used in the AIMP configuration. A concept was proposed, a decision to fly the contamination experiment on AIMP-E was made, and with the cooperation of others, a qualified flight unit was delivered in two months.

GENERAL DESCRIPTION

The contamination monitor shown in Figure 1 is a 4.5-inch-wide, 5.5-inch-long, 4.375-inch-high instrument which weighs approximately 737 grams. The monitor is capable of operating with the spacecraft's unregulated voltage of 14 to 19.6 volts and at 15 volts uses approximately 210 milliamps. Figure 2 is a schematic of the contamination monitor electronics and optics. The housing for the electronics is made of aluminum 6061 alloy with stainless steel set screws. The solar cells and the lamp housing are supported by a laminated plastic tubing which has a high-physical strength glass fabric base with excellent heat resistance and dimensional stability.

The monitor uses a stable subminiature 5000-hour-life, 2.5-volt, 0.4-amp lamp which has a nominal light output of 800 foot-candles through a three-sixteenth-inch-minimum-diameter window three-eighths of an inch from the lamp tip. This lamp has an integral lens and is 0.240 inch in diameter.

OPERATIONAL CONSIDERATIONS

In the monitor, the lamp was used at 0.25 volt below its rated voltage value which increased its life expectancy to 13,500 hours. This assured ample lamp life for the duration of the experiment. All lamps were carefully inspected for filament location and uniformity of the lens end to ensure proper image-forming effects. Figure 3 shows the spectral response of the lamps used. The lamp was mounted in a glass-laminated plastic sleeve with a room-temperature vulcanizing (RTV) silicone adhesive. The lamp-mounting sleeves were baked in a vacuum oven to eliminate any possibility of the sleeves discharging contamination during the experiment. The optical axis of the lamp and the mechanical axis of the sleeve were aligned in a lathe. To maintain the fixed-optical-mechanical-axis alignment, the assembly was supported within a plastic sleeve of a larger diameter and held firmly in place with stainless steel set screws.

The signal optics consist of two illuminating double-convex lenses, 18-mm diameter, with a back and front focal length of about 20 mm. These lenses were

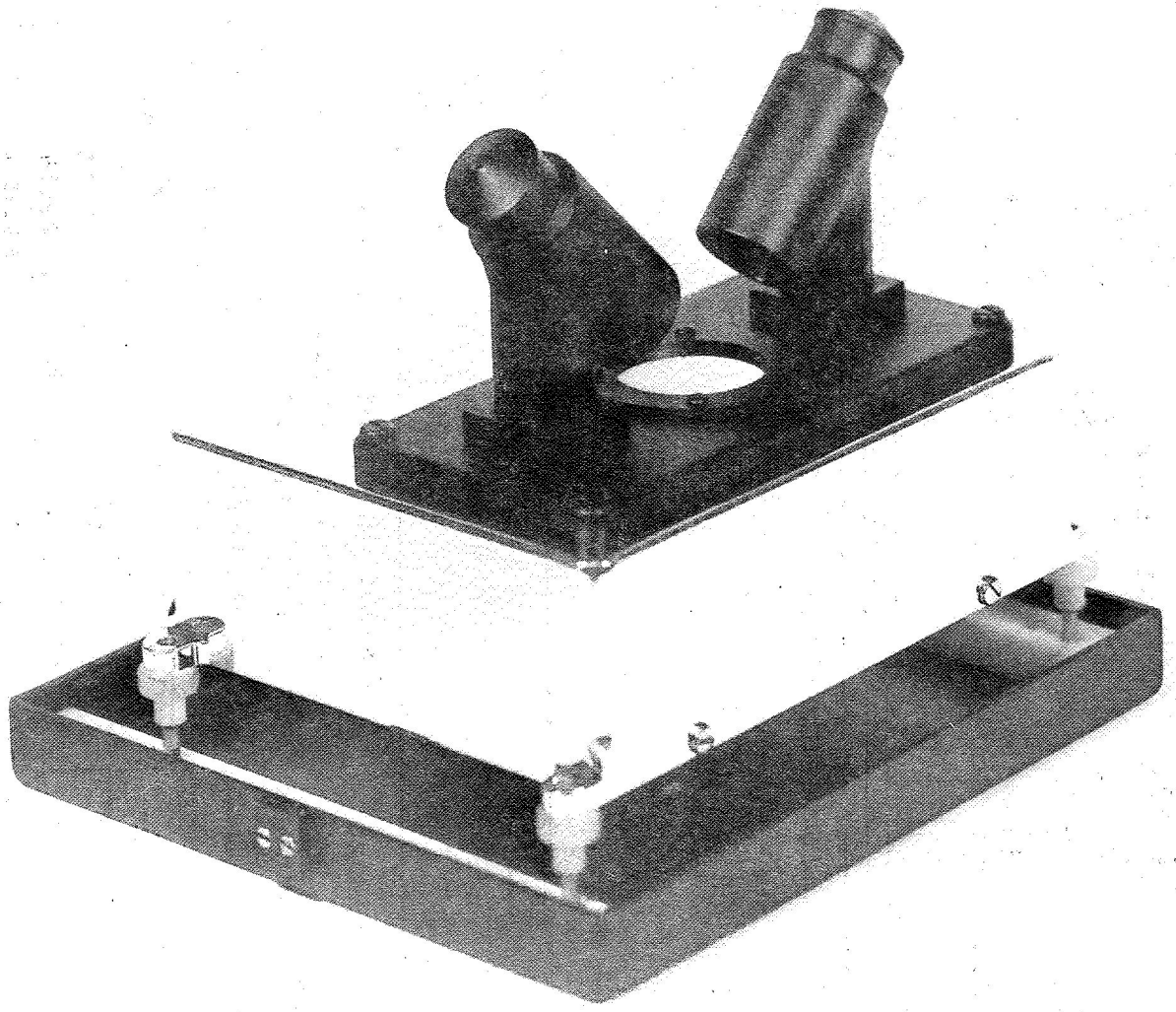

Figure 1. Contamination Monitor

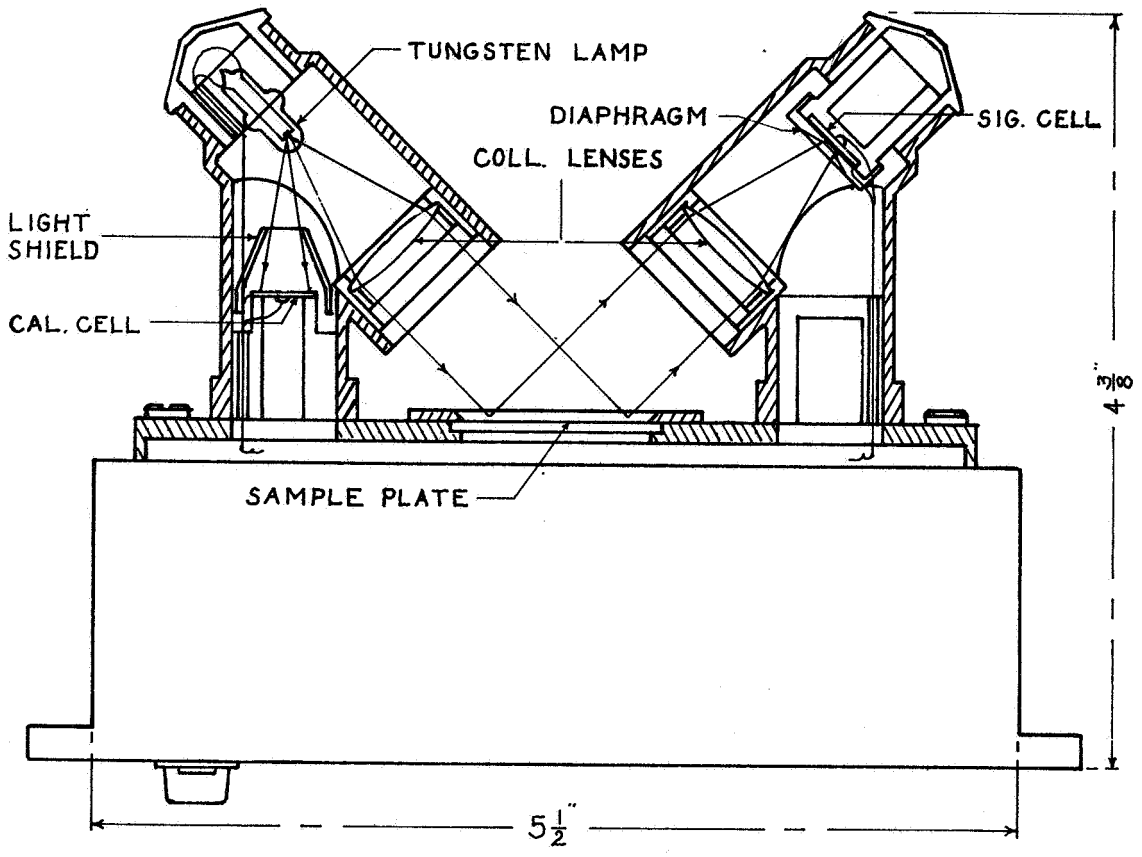

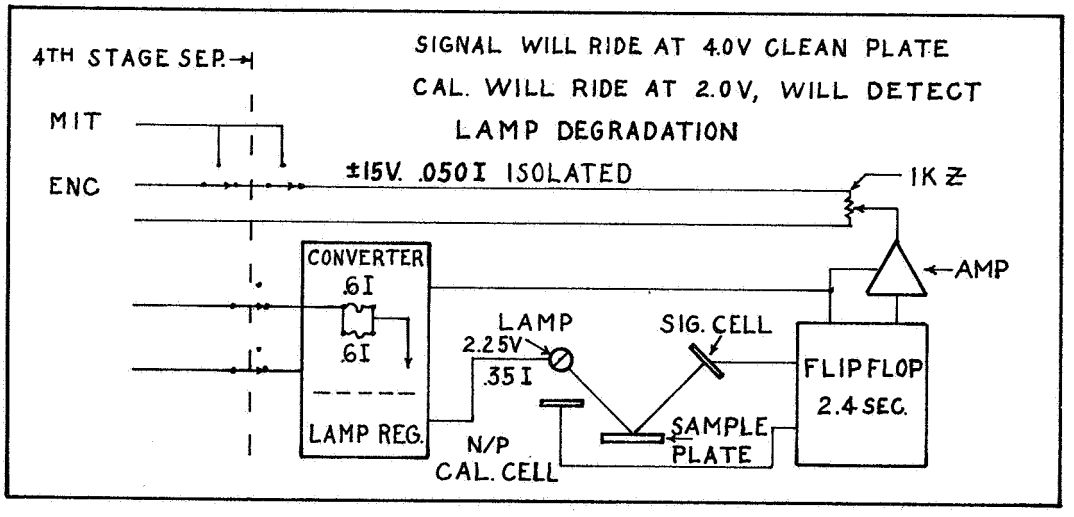

Figure 2. Contamination Monitor Schematic

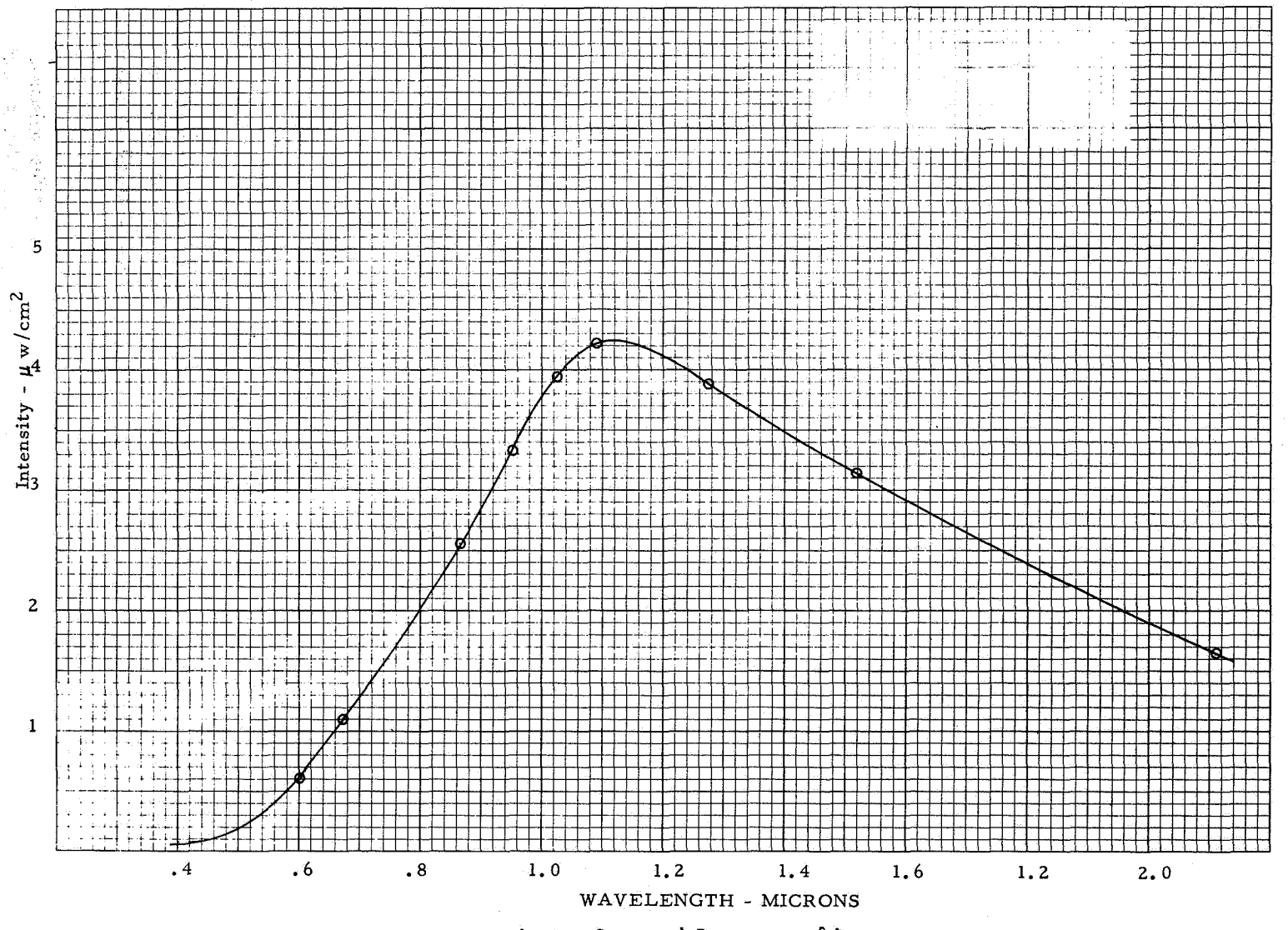

Figure 3. Relative Spectral Response of Lamps

coated with magnesium-fluoride to increase their light transmission and improve the instrument's efficiency. The light from the lamp was transmitted through one lens, illuminating the sample plate which was a substrate of highly buffed aluminum with a stable evaporated aluminum coating applied to increase its reflectance. The surface, which has a nominal reflectance of 90 percent, reflects the illuminating light impinging on it, and transmits it through the second lens which converges and focuses the light image on the signal cell, uniformly covering an aperture of 1-1/2 mm diameter. The signal cell is protected from stray light by a diaphragm which covers it entirely except for a 2-mm aperture in the center while the calibration cell has a conical light shield. The signal cell and calibration cell are 1 x 1 cm n-on-p silicon cells and have a spectral response as shown in Figure 4. Due to its location in the instrument, the calibration cell enclosed with the light source just sees a portion of the transmitted light from the lamp and provides an inflight calibration. By adjusting the position of the calibration and signal cells, limited control of their individual response is obtainable. Solar cells were used in near short circuit condition so as to achieve maximum thermal stability over the temperature range of interest (-20 to +50° C). To differentiate between the calibration and signal cell outputs, the calibration cell was positioned to provide only one-half the output of the signal cell for the uncontaiminated sample condition.

The signals were multiplexed to accommodate the two sensor outputs on one available telemetry channel. The multiplexer circuit consists of two unijunction transistors and two relays (Figure 5). The signals are switched every 2.4 seconds (±10 percent) to provide a full frame of each signal in the display of the spacecraft telemetry format. Duration sampling time was obtained through careful resistor selections.

The amplified calibration cell output is 2 volts; the amplified signal cell output is 4 volts, when the sample surface is uncontaminated.

Any deposit on the sample surface will affect the amplified output of the signal cell with no effect on the calibration signal cell output.* A decrease in voltage output of the signal cell caused by contamination deposited on the sample surface will indicate that the original reflectance was attenuated. The calibration cell could be changed by a displacement or deforming of the filament within the lamp; such a change would also affect the output response of the signal cell. Figure 6 shows the variation of output signal created by a deposit of contamination. This figure indicates that the percent decrease in reflectance is linearly proportional to the increase in output signal (voltage).

*If the reflecting surface were to become heavily contaminated so that it had a strong diffuse reflectance component, it would be possible for some light to be reflected back into the light source tube. A small fraction of this light might reach the calibration cell and introduce a small error.

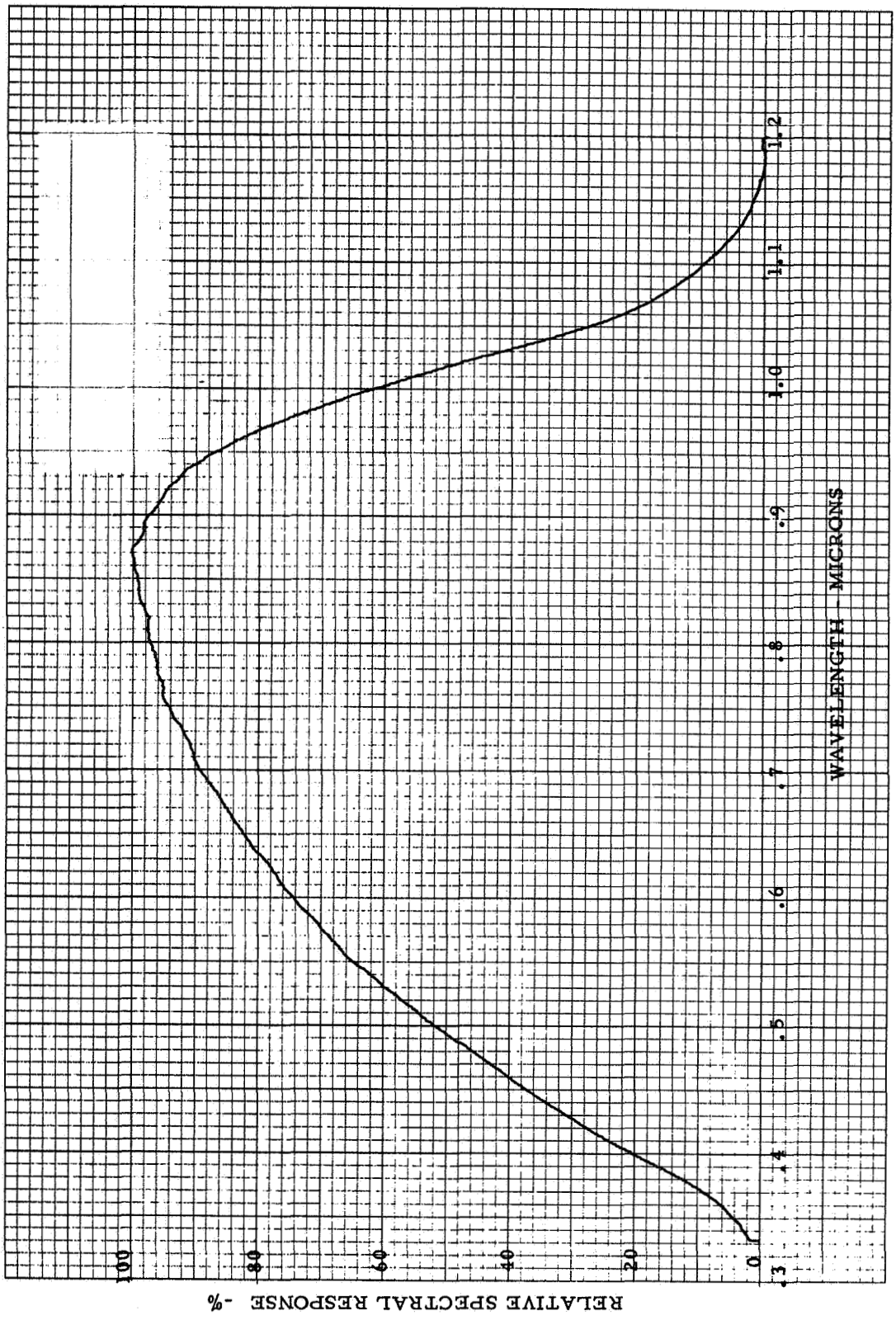

Figure 4. Contamination Monitor Relative Spectral Response N-on-P Silicon Solar Cell

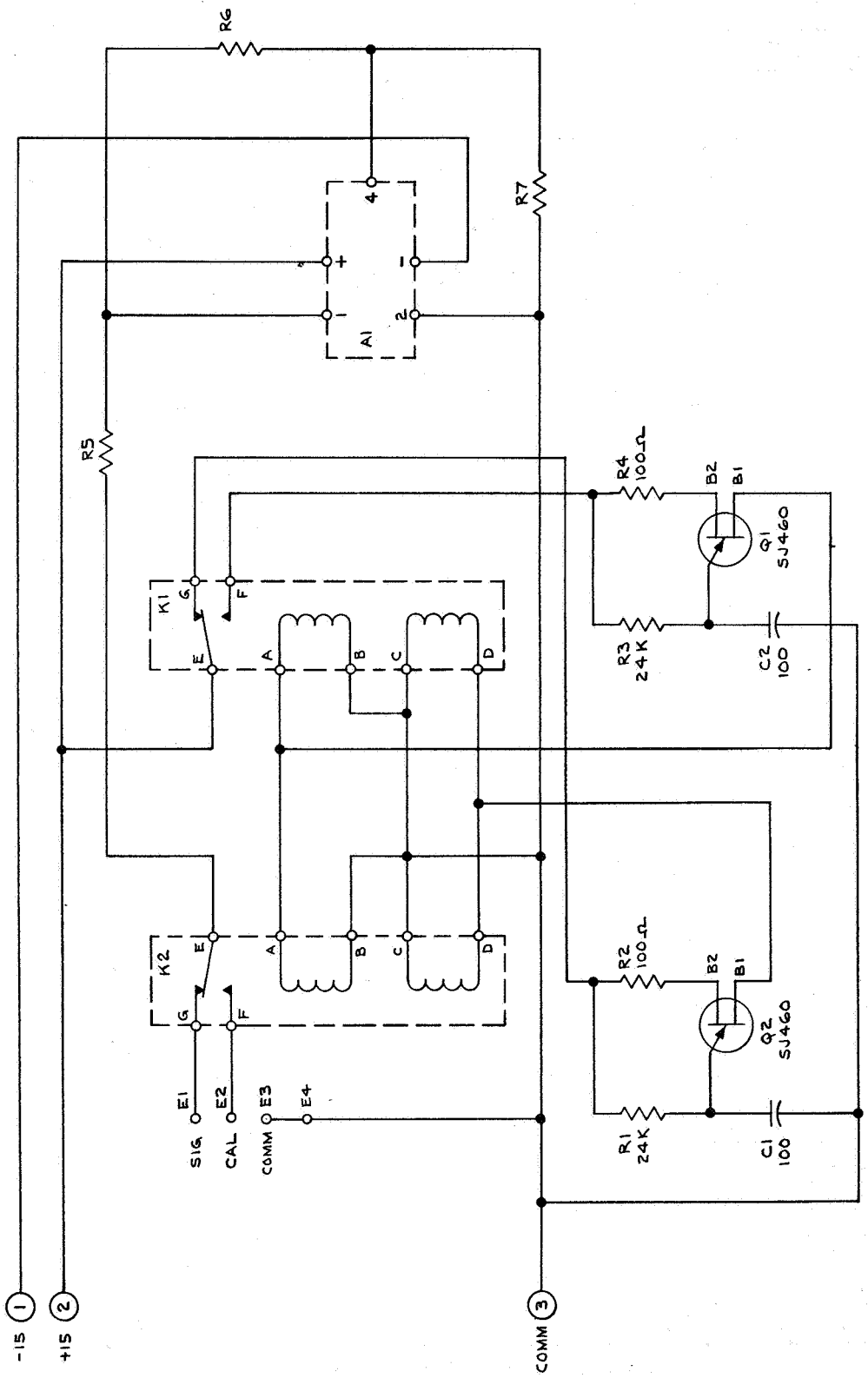

Figure 5. Operational Amplifier Schematic Diagram

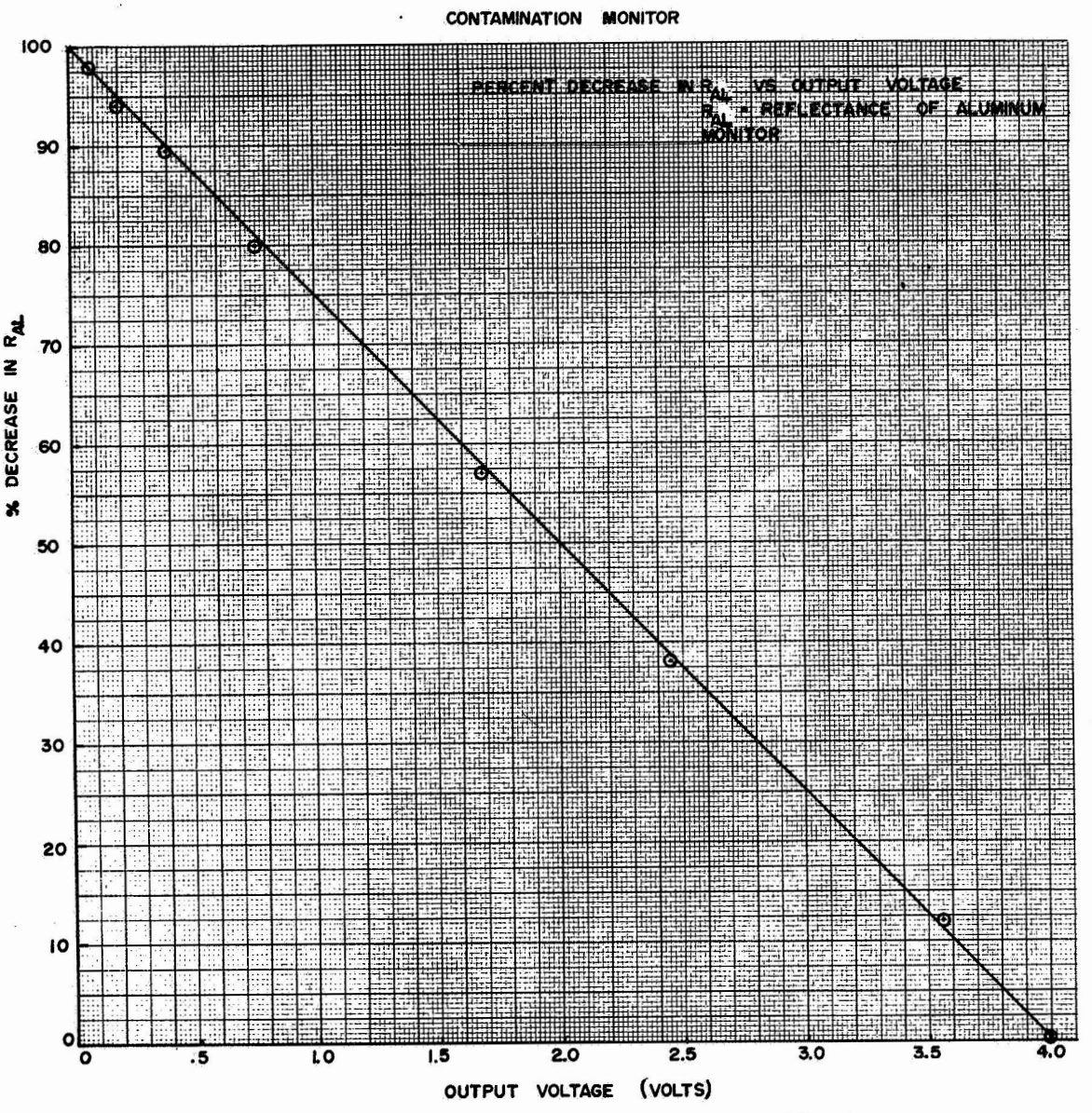

Figure 6. Percent Decrease in Reflectance of Aluminum (R_{AL}) Versus Output Voltage

Figure 7 shows a portable operational test set designed and fabricated to accommodate the contamination monitor, and used to determine the decrease in output-signal voltage with varying amounts of contamination. The test set was also used to simulate the fluctuations in spacecraft voltage (14 to 19.6 volts) to check instrument reliability under actual conditions. The test set operates on 115 vac which it converts to the required dc voltages; a 0-to-25-vdc meter indicates the voltage applied to the monitor, and a 0-to-500-ma meter indicates the current through the monitor. Signal and calibration voltage can be displayed on a self-contained digital voltmeter, or patched into an external strip-chart recorder.

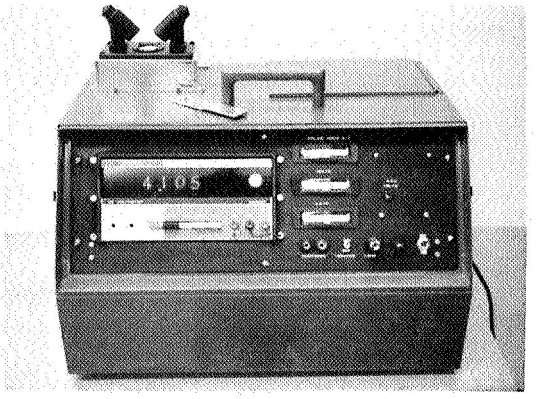

Figure 7. Contamination Monitor Test Set

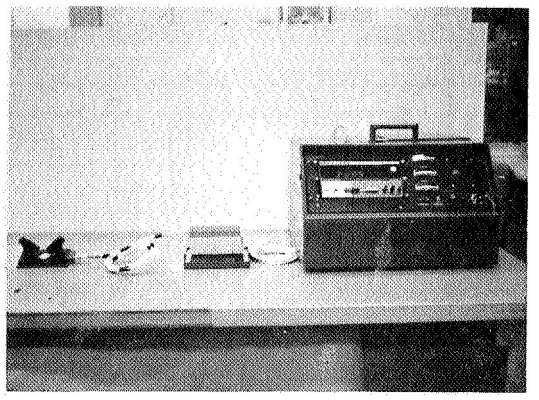

Figure 8. Remote Operature

To permit remote simulated-environment monitoring of the sensor during mock countdown tests of OGO-D and -E, one contamination monitor was modified by separating the optical portion and the electronics portion and connecting them by a cable (Figure 8). Remote monitoring was required because access ports in the fairing are too small to accommodate the complete contamination monitor.

The experiment output signal is connected to the telemetry channel by a pair of switches which are activated by the presence of the retrorocket motor mounted on the spacecraft. The switches assure a high-reliability switchover from the contamination monitor telemetry output to the MIT experiment telemetry output upon ejection of the retrorocket case (Figure 9).

A converter-regulator was designed to provide a highly stable +2.25 vdc at 360 ma for the lamp and +15 vdc and -15 vdc for the operational amplifier. The two 15 vdc outputs had a voltage tolerance of ±1 percent and each delivered 25 ma. Figure 10 shows a schematic drawing of the converter-regulator. Figure 11 shows the converter-regulator with the operational amplifier mounted on the printed circuit board.

Typical characteristics of the converter-regulator are as follows:

Regulation: Temperature - -20° C to +70° C
Volts input - 13 vdc to 20 vdc

±15 vdc - ±0.9 percent
2.25 vdc - ±0.085 percent

For the temperature range of 0° C to 40° C, which was of primary interest and the previously stated ΔVin, the 2.25 vdc line had a regulation of ±0.038 percent.

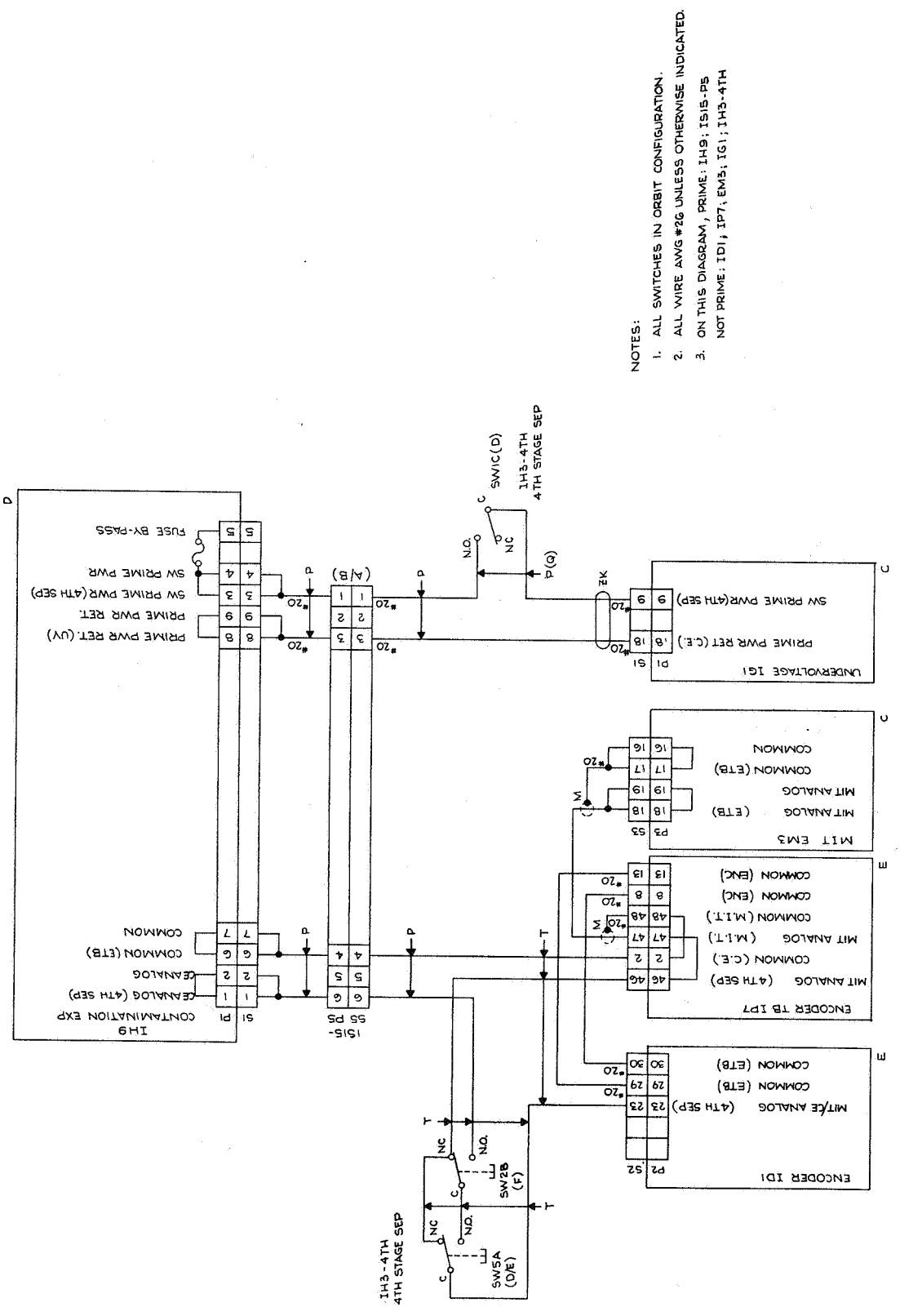

Figure 9. Contamination Experiment Cable Diagram

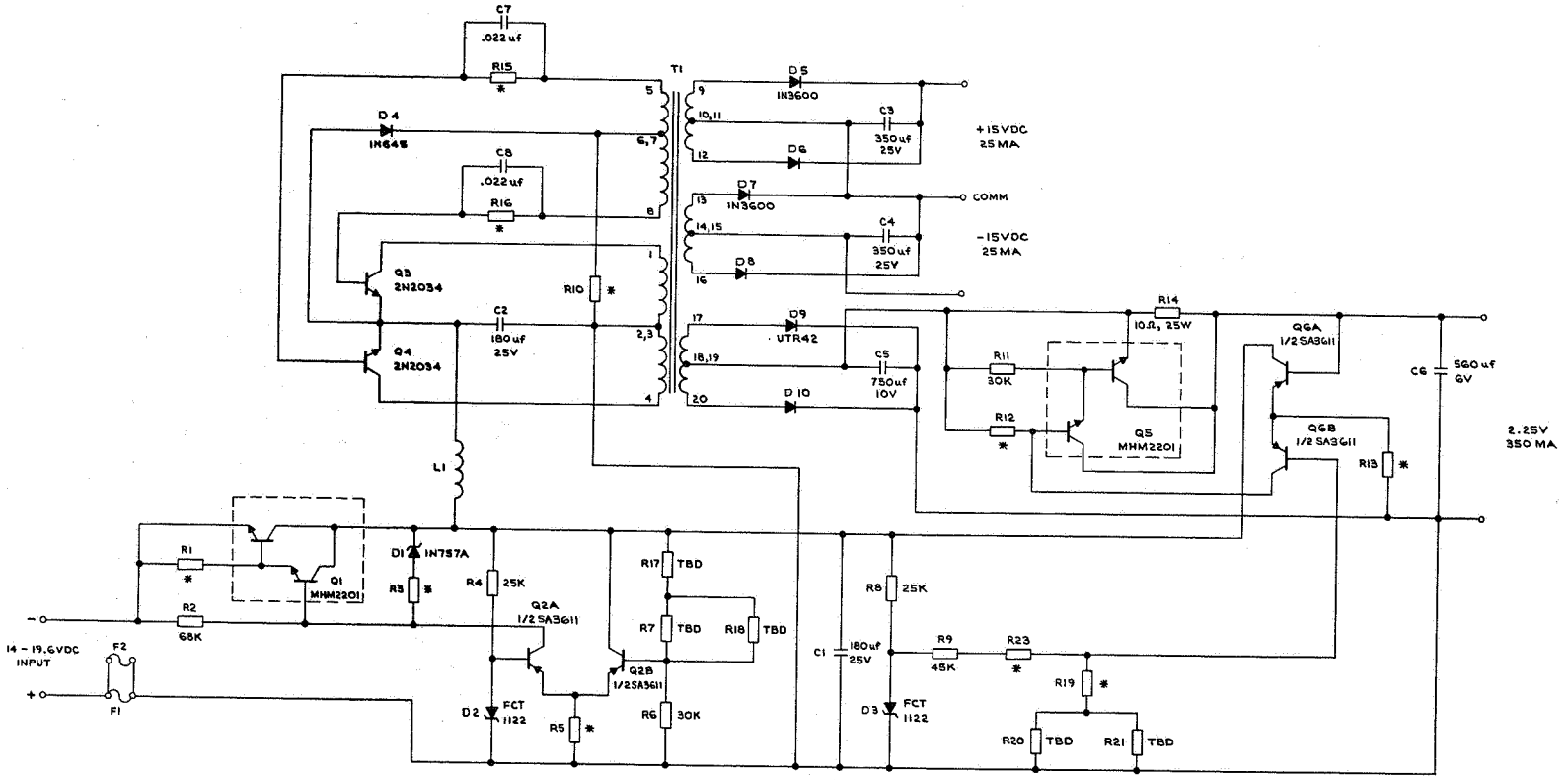

NOTES:
1. ALL RESISTORS 1/4 W, 1% OR SMALLER (PHYSICAL SIZE). * = SEE CHART FOR VALUE.
2. C3, C4, AND C5 ARE 137D W CASE, ALL OTHERS T CASE.

LAST CIRCUIT SYMBOL USED:

R23	T1
Q6	L1
C8	F2
D 10	

COMPONENT	UNIT SERIAL NUMBER				
	Q1	Q2	Q3	Q4	Q5
R1	30K	30K	30K	56K	56K
R3	100K	100K	100K	75K	62K
R5	45.3K	45.3K	45.3K	45.3K	30.9K
R10	5K	5K	6.8K	6.2K	6.2K
R12	NONE	150K	150K	150K	68K
R13	39.2K	21.5K	45.3K	20K	20K
R15	75Ω	75Ω	75Ω	100Ω	110Ω
R16	75Ω	75Ω	75Ω	100Ω	110Ω
R19	100Ω THER-MISTOR	JUMPER	JUMPER	JUMPER	JUMPER
R23	JUMPER	2.7K SEN-SISTOR	2.2K SEN-SISTOR	1.8K SEN-SISTOR	1.5K SEN-SISTOR

Figure 10. Converter Regulator Contamination Monitor

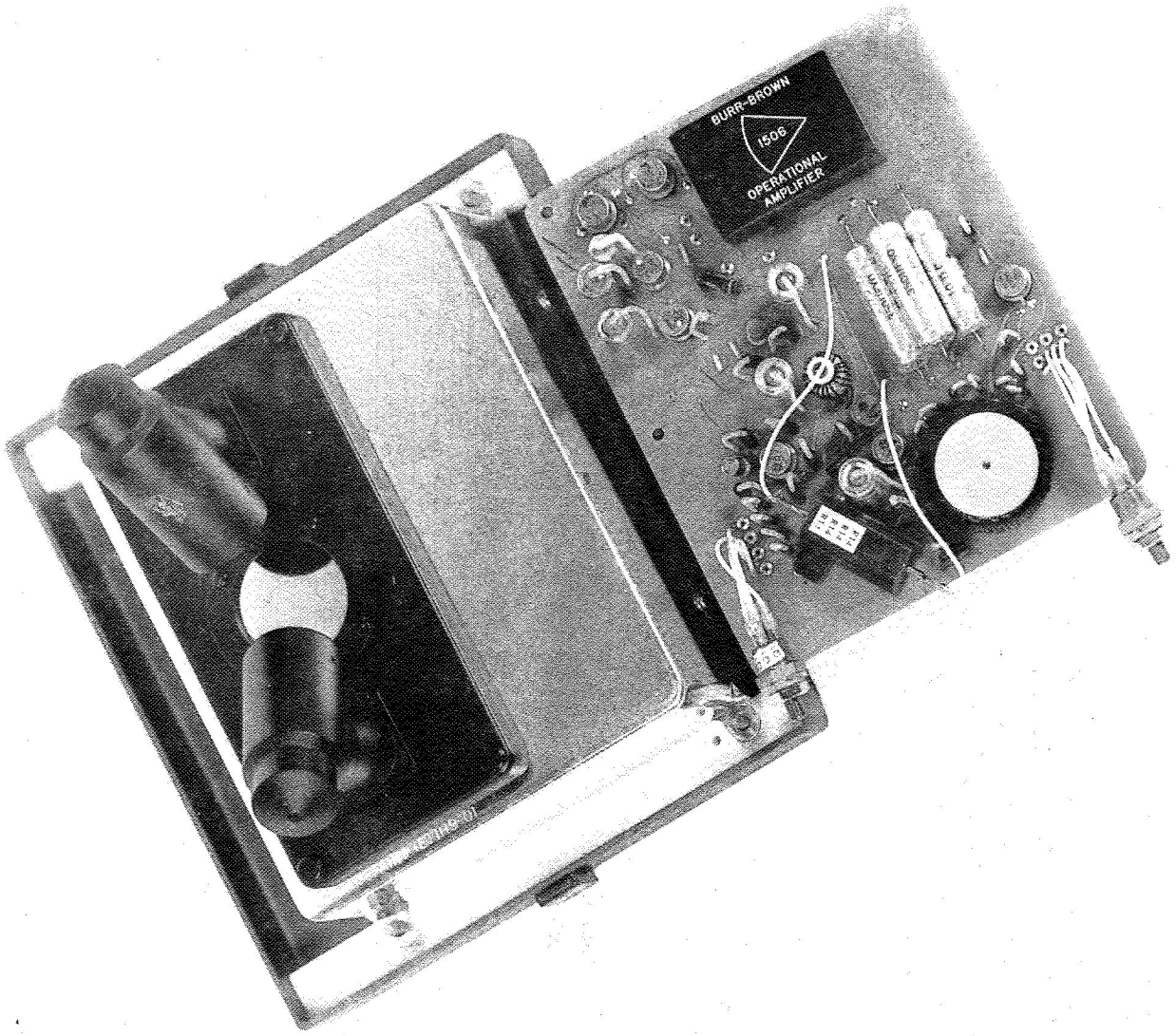

Figure 11. Converter-Regulator and Amplifier

Efficiency:	19.6 v input	30 percent
	14 v input	42 percent

Figure 12 shows the output of the 2.25-vdc regulator as a function of temperature for flight units SN 04 and SN 05.

PERFORMANCE AND RESULTS

The contamination monitor was flown on the AIMP-E satellite which was launched on July 19, 1967. The flight experiment lasted 68 hours, 57 minutes, and 57 seconds, from launch to fourth-stage separation. During this time the experiment used analog telemetry frame 6 which was not used by the MIT experiment during the transfer trajectory phase; after fourth-stage separation, the instrument's data line was switched to MIT analog output. Figure 14 shows the AIMP sequence of events from launch through data-line switchover. Figure 13 shows the location of the monitor aboard the satellite.

An analysis of the flight-performance data shows that the instrument performed as expected. The sampled-surface signal and the light-source-calibration signal were sampled, alternately and continuously, during the flight time allotted to the monitor.

The signal and calibration modes, observed before launch to be stable, exhibited no changes during ignition or burn of the main engine or solid motors.

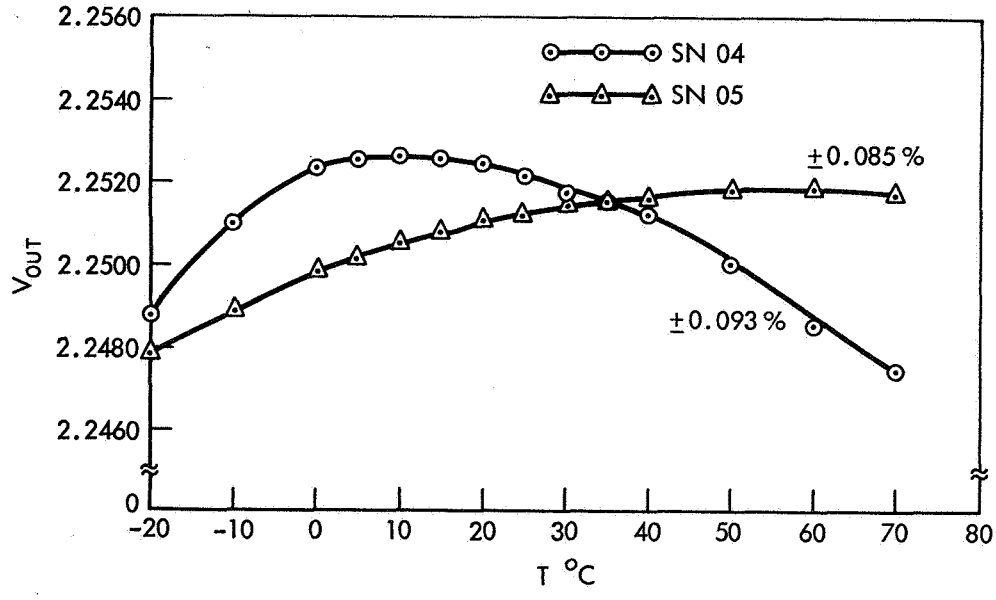

Figure 12. 2.25-VDC Regulator Output Versus Temperature

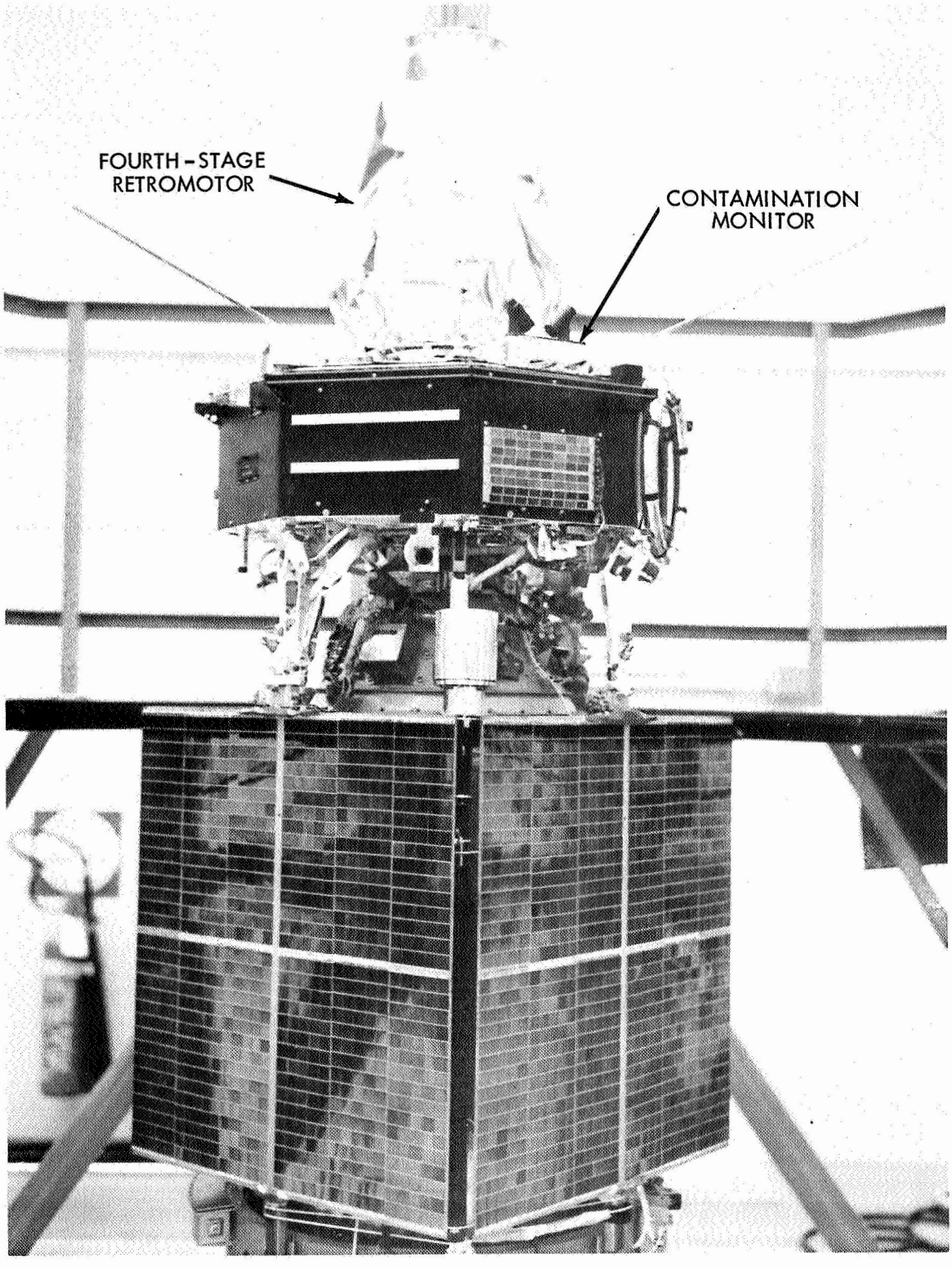

Figure 13. Location of Contamination Monitor on Satellite

REPRESENTATIVE AIMP-E LAUNCH SEQUENCE

SEQUENCE NO.	TIME/SEC	EVENT
1	0	STAGE I LIFTOFF
2	150	MAIN ENGINE CUTOFF
3	155	STAGE II IGNITION SIGNAL
4	155	STAGE I / II SEPARATION
5	216	JETTISON FAIRING
6	537	STAGE II CUTOFF
7	601	START COAST PHASE PITCH PROGRAM
8	800	END COAST PHASE PITCH PROGRAM
9	1006	FIRE SPIN ROCKETS (SPIN UP)
10	1008	JETTISON STAGE II - ACTIVE RETRO SYSTEM
11	1021	STAGE III IGNITION
12	1052	STAGE III BURNOUT
13	1081	DE-SPIN STAGE III / SPACECRAFT
14	1096	SOLAR CELL PADDLE RELEASE (4)
15	1106	FLUXGATE BOOM RELEASE (2)
16	1136	SPACECRAFT/STAGE III SEPARATION - YO STAGE III
17		SPIN STABILIZED COAST
18	DBC	COMMAND TIMER
19	DBC + T	DIRECT COMMAND STAGE IV IGNITION
20	DBC + T + 22	STAGE IV BURNOUT
21	DBC + T + 22 + 7200	SEPARATE STAGE IV
22		CONTAMINATION MONITOR DATA LINE SWITCHED TO MIT ANALOG OUTPUT
23		IN ORBIT

T = TIMER

DBC = DETERMINED BY COMPUTER

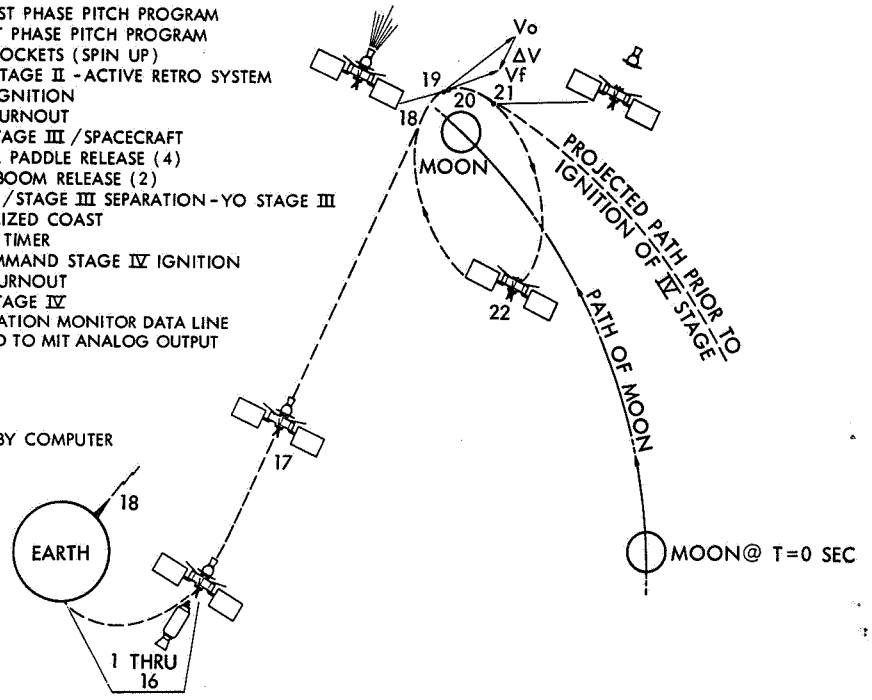

Figure 14. Typical Flight Plan

No change means that there was no detectable contamination during the launch phase of the satellite, either from vehicle operation or from the aerodynamic heating of the fairing. Oscillation of the filament in the light source occurred at T+280 seconds and continued to T+444 seconds into the flight, when the second stage was in its burn phase. This oscillation was expected because the monitor exhibited this tendency during vibration tests at GSFC. The oscillation of the filament in the light source affected the calibration cell more severely than it affected the signal cell. This oscillation was also verified in the analog telemetry readout of AIMP-E spacecraft.

The satellite then went into a period when the telemetry was not received. When the telemetry was restored, the sensor signal and calibration signal values returned to normal and remained stable throughout the flight, except for a slight drop in signal caused by reduced temperature. The calibration and the signal were stable during and after the attitude-control system maneuver, indicating no deposit of contamination.

After fourth-stage firing, the monitor telemetry indicated contamination. Contamination was detected on the instrument's sensor surface approximately 3 minutes and 25 seconds after fourth-stage ignition. The contamination continued to build up; it reached total accumulation 15 minutes later. At 6 minutes and 8 seconds after fourth-stage ignition, a large drop in sensor signal was noted. This was a temporary condition which might be attributed to a gas cloud or another transient condition.

The deposit was a steady accumulation which could be associated either with increased bottle temperature (causing outgassing of surrounding materials) or with the deposit of residual gases from the spent bottle. The gross accumulation took place within 18 minutes and 25 seconds after fourth-stage ignition. The total deposit remained on the surface for 43 minutes and 38 seconds, after which the nominal absorptance* decreased slightly, then remained constant throughout the life of the experiment. The decreased absorptance could have been caused by a partial migration of contamination from the experiment sensor surface.

The nominal absorptance changed from 10 to 23.5 percent; the effect of the deposited material more than doubled the original absorptance characteristic of the sensor surface.* The instrument had no capability to determine the change in emittance characteristics of the deposited material. Figure 15 shows the instrument's performance during the critical portion of the flight in which contamination was deposited. The graph also indicates the change in the bottle temperature of the fourth-stage motor during this period. Table 1 lists events of interest

*Absorptance as used here is not solar absorptance. The source of illumination is a tungsten lamp with peak energy near 9000 angstroms; the detector is a silicon solar cell with peak response near 9000 angstroms and negligible response below 4000 and above 12000 angstroms.

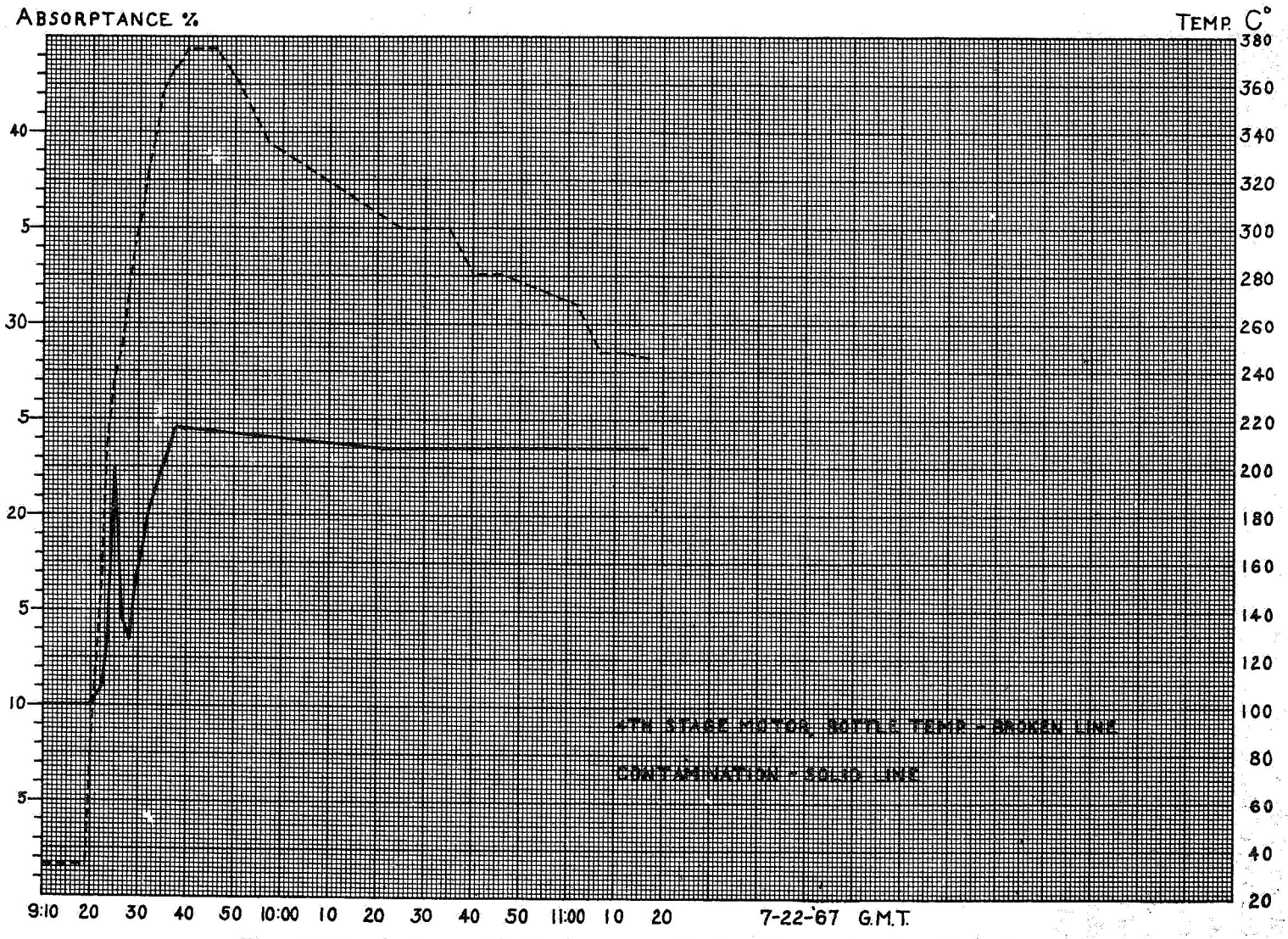

Figure 15. Instrument's Performance During Contamination Deposits

Table 1
Flight Performance Events

Date (1967)	Time (GMT)			Events	Comb-Filter Numbers Analog Mode		Freq. Conv. to Voltage		Comments	Absorptance* (%)	4th-stage Hi-bottle Temp. (°C) ±25°C
	hr	min	sec		Cal	Sig	Cal	Sig			
7-19	14	14	38	Spacecraft on internal power	068	027	2.10	4.15	Ana. tape 005 frame 6		
200	14	16	00		068	027	2.10	4.15			
	14	17	22		068	027	2.10	4.15			
	14	18	44		068	027	2.10	4.15			
	14	19	01	Launch							
	14	20	06		068	027	2.10	4.15			
	14	21	31	Main eng. cutoff							
	14	21	35	2nd-stage ignition							
	14	22	37	Fairing separation							
	14	22	49	2nd-stage burn phase	063	026	2.35	4.20	Filament osc. light source		
	14	24	11	2nd-stage burn phase	059	026	2.55	4.20	Filament osc. light source		
	14	25	33	2nd-stage burn phase	061	026	2.45	4.20	Filament osc. light source		
	14	26	50	Blackout							
	17	18	40	Reduced temp., unit stable	068	030	2.10	4.00	No detectible contamination Ana. tape 008 frame 6	10	
	23	18	41	Transfer trajectory phase	068	030	2.10	4.00	Ana. tape 009	10	
7-20	07	18	38	Transfer trajectory phase	068	030	2.10	4.00	Ana. tape 011	10	
201	15	18	35	Transfer trajectory phase	068	030	2.10	4.00	Ana. tape 014	10	
	23	18	32	Transfer trajectory phase	068	030	2.10	4.00	Ana. tape 017	10	
7-21	03	28	54	Transfer trajectory phase	068	030	2.10	4.00	ACS off	10	
202	03	30	16	Transfer trajectory phase	068	030	2.10	4.00	ACS off	10	
	03	31	38	Transfer trajectory phase	068	030	2.10	4.00	ACS on	10	
	03	32	59	Transfer trajectory phase	068	030	2.10	4.00	ACS off	10	
	03	34	21	Transfer trajectory phase	068	030	2.10	4.00	ACS off	10	
	07	18	29	Transfer trajectory phase	068	030	2.10	4.00	Ana. tape 019 frame 6	10	
	15	18	26	Transfer trajectory phase	068	030	2.10	4.00	Ana. tape 021	10	
	23	18	23	Transfer trajectory phase	068	030	2.10	4.00	Ana. tape 023	10	
7-22	07	18	20	Transfer trajectory phase	068	030	2.10	4.00	Ana. tape 026	10	24
203	09	12	52	Transfer trajectory phase	068	030	2.10	4.00	Ana. tape 027	10	28
	09	14	14	Transfer trajectory phase	068	030	2.10	4.00	Ana. tape 027	10	28
	09	15	36	Transfer trajectory phase	068	030	2.10	4.00	Ana. tape 027	10	28
	09	16	57	Transfer trajectory phase	068	030	2.10	4.00	Ana. tape 027	10	28
	09	18	19	Transfer trajectory phase	068	030	2.10	4.00	Ana. tape 027	10	28
	09	19	00	4th-stage ignition							28
	09	19	41		068	030	2.10	4.00	Ana. tape 027 frame 6	10	33
	09	20	03		068	030	2.10	4.00	Ana. tape 027 frame 6	10	80
	09	22	25	Outgassing	068	031	2.10	3.95	Contamination	11.1	160
	09	23	27	Outgassing	068	033	2.10	3.85	Contamination	13.4	205
	09	25	08	Outgassing	069	041	2.05	3.45	Cloud effect gross contamination	22.4	236
	09	26	30	Outgassing	068	034	2.10	3.80	Ana. tape 027 contamination	14.5	250
	09	27	52	Outgassing	068	033	2.10	3.85	Ana. tape 027 contamination	13.4	274
	09	29	14	Outgassing	068	035	2.10	3.75	Ana. tape 027 contamination	16.7	294
	09	30	36	Outgassing	068	037	2.10	3.65	Ana. tape 027 contamination	17.9	306
	09	31	57	Outgassing	068	039	2.10	3.55	Ana. tape 027 contamination	20.1	325
	09	33	19	Outgassing	068	040	2.10	3.50	Ana. tape 027 contamination	21.25	340
	09	34	41	Outgassing	068	041	2.10	3.45	Ana. tape 027 contamination	22.4	356
	09	36	03	Outgassing	068	042	2.10	3.40	Ana. tape 027 contamination	23.5	362
	09	37	25	Outgassing	068	043	2.10	3.35	Total accumulation	24.6	367
	09	38	46		068	043	2.10	3.35		24.6	370
	09	40	08		069	043	2.05	3.35	Ana. tape 027	24.6	375
	09	41	30		068	043	2.10	3.35	Ana. tape 027	24.6	375
	09	42	52		068	043	2.10	3.35	Ana. tape 027	24.6	375
	09	44	14		068	043	2.10	3.35	Ana. tape 027	24.6	375
	10	21	03	Film migration	068	042	2.10	3.40	Ana. tape 027	23.5	304
	11	16	57		068	042	2.10	3.40	Last sequence received	23.5	246
	11	17	00	Fourth-stage separation							

(with comments) throughout the flight. The distribution of contamination on the satellite surfaces was not necessarily uniform; the degree of contamination reported by the sensor surface was representative only of its location, on the top cover of the AIMP-E satellite.

RECOMMENDATIONS

Shield the spacecraft against deposits of contamination on the surfaces or jettison the fourth-stage motor casing as soon as practicable, preferably within 3 minutes after burnout, to avoid contamination.

ACKNOWLEDGEMENTS

The initial evaluation of electronics (instrumentation electronics support) and the operational amplifier used for the contamination monitor were furnished by Harry Leverone and Nathan Mandell, Instrumentation Section, Test and Evaluation Division, Goddard Space Flight Center.

The converter-regulator for the contamination monitor was designed, tested, and furnished by Joseph A. Gillis, Jr., Space Power Technology Branch, Spacecraft Technology Division.

REFERENCES

1. Gillis, Joseph A.: High Regulation Contamination Monitor Converter Regulator for IMP-E. I Document 716-67-147. NASA, Goddard Space Flight Center. April 1967.